Copyright © 2009 by ABCM

KINEMATIC MODEL FOR ECLIPSE AND ECLIPSE-II PARALLEL ROBOT

Henrique Simas, hsimas@univali.br
UNIVALI – CE São José, Rod. SC 407, km 04 , Sertão do Imaruim São José, SC, CEP 88022-000

Altamir Dias, altamir@emc.ufsc.br
Daniel Martins, daniel@emc.ufsc.br
EMC - Universidade Federal de Santa Catarina – Campus Trindade, Florianópolis – SC, CEP 88040-970

Abstract. *In general, the inverse kinematics of robots is solved by analytical methods, which are based on geometric intuition. As the kinematic structure of the robot grows complex, however, geometric intuition sometimes fails. This is the typical case of parallel robots. Some work present analytical solutions for the inverse kinematics of parallel robots, but in general their kinematics are conceptually simple. Eclipse and Eclipse-II are parallel robots with complex kinematic chains, and their inverse kinematics is obtained analytically using geometric analysis for some particular configurations only. This paper proposes a method to model differential kinematics for these two particular robots using the Assur virtual chains method. This method allows to systematize inverse kinematics resolution and to apply a numerical integration method with closure error control. Screw theory, Davies method, Assur virtual chains and the numerical integration, which are the fundamentals of the method, are shortly reviewed. A study of singularities is made, and a simulation of a planned trajectory to illustrate the proposed model is presented.*

Keywords*: Parallel robots, complex kinematic chains, Assur virtual chain, singularity analysis.*

1. INTRODUCTION

The study of parallel mechanisms is currently an area of interest for industrial applications and research. Advances in computing technology, allied to the development of more accurate analysis methods, motivates an increasingly adoption of parallel robots in production systems.

This paper discusses a solution for the inverse position and velocity kinematics of the Eclipse and Eclipse-II parallel robots. The Eclipse robot was presented by Kim and Park (1998), based on design study of a kinematic structure capable of execute 360^o operations in the workspace. Eclipse-II was first presented in 2002 (Kim *et al*, 2002), as an evolution of the Eclipse robot aimed to be used in flight simulators, because of the 360^o movement feature.

These papers presented the forward and inverse kinematics of these robots based on geometric approach, and this was also the case of their singularity analysis. Some work presented alternative solutions, but were also based on geometry (Liu *et al*, 2003; Altuzarra *et al.*, 2004). Other references treat just the forward kinematics (Wang, 2006). The proposed methods used to obtain the differential kinematics were not systematic, and they were used in particular situations in each case.

In parallel robots, singular configurations occur in both forward and inverse kinematics (Gosselin and Angeles, 1990). Their identification can be made through kinematic differential models, which must be consistent, to make their analysis possible. Singularity is discussed using geometric analysis (Gregorio, 2005), and Altuzarra *et al.* (2004) presents a singularity classification for closed kinematic chains.

This work proposes a systematic model to differential kinematics of the Eclipse and Eclipse-II robots using the method of Assur virtual chains (Campos *et al*, 2005). The virtual chains allowed the development of an integration method with closure error measured control (Simas, 2008), which is reviewed here. This paper also presents the differential model, a study of singularities and a simulation of a planned trajectory to validate the proposed model.

This paper aims to contribute with the study of parallel robots kinematics, by demonstrating a method which can be used in a systematic way in the Eclipse and Eclipse-II robots, and also by presenting a method to analyze singularities.

2. THEORETICAL REVIEW

The description of the Eclipse and Eclipse-II differential kinematics is based on screw representation and in Assur virtual chains. Davies' method is used to obtain the inverse kinematics of closed chains, while graph analysis allows investigation of the relationship of movement in a joint. These concepts are shortly described in the following.

2.1. Screw representation of differential kinematics

The general spatial differential movement of a rigid body consists of a differential rotation about, and a differential translation along an axis named the instantaneous screw axis. In this way the velocities of the points of a rigid body with respect to an inertial reference frame *O-xyz* may be represented by a differential rotation ω about the

instantaneous screw axis and a simultaneously differential translation τ about this axis. The complete movement of the rigid body, combining rotation and translation, is called screw movement or twist and is here denoted by $\$$. Figure 1 shows a body "twisting" around the instantaneous screw axis. The ratio of the linear velocity to the angular velocity is called the pitch of the screw $h=||\tau||/||\omega||$.

The twist may be expressed by a pair of vectors $\$ = \left[\omega^T ; V_p^T\right]^T$, where ω represents the angular velocity of the body with respect to the inertial frame and V_p represents the linear velocity of a point P attached to the body which is instantaneously coincident with the origin O of the reference frame. A twist may be decomposed into its magnitude and its corresponding normalized screw. The twist magnitude $\dot{q}$ is either the magnitude of the angular velocity of the body, $||\omega||$, if the kinematic pair is rotative or helical, or the magnitude of the linear velocity, $||V_p||$, if the kinematic pair is prismatic. The normalized screw $\hat{\$}$ is a twist of unitary magnitude, i.e.

$$\$ = \hat{\$}\dot{q} \tag{1}$$

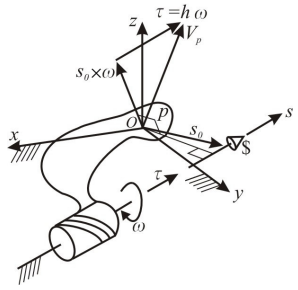

Figure 1. Screw movement or twist.

The normalized screw coordinates (Davidson and Hunt, 2004) are written as

$$\hat{\$} = \begin{bmatrix} s \\ s_0 \times s + hs \end{bmatrix} \tag{2}$$

where vector $s=[s_x\ s_y\ s_z]^T$ denotes an unit vector along the direction of the screw axis, and vector $s_o=[s_{ox}\ s_{oy}\ s_{oz}]^T$ denotes the position vector of a point lying on the screw axis.

Thus, the twist in Eq. (1) expresses the general spatial differential movement (velocity) of a rigid body relative to an inertial reference frame *O-xyz*. The twist can also represent the movement between two adjacent links of a kinematic chain. In this case, twist $\$_i$ represents the movement of link i relative to link $(i-1)$.

2.2. Davies' method

Davies' method is a systematic way to relate the joint velocities in closed kinematic chains. Davies (Campos *et al*, 2005) derived a solution to the differential kinematics of closed kinematic chains from Kirchhoff circulation law for electrical circuits. The resulting Kirchhoff-Davies circulation law states that "The algebraic sum of relative velocities of kinematic pairs along any closed kinematic chain is zero" (Campos *et al*, 2005).

This method is used to obtain the relationship between the velocities of a closed kinematic chain. Since the velocity of a link with respect to itself is null, the circulation law can be expressed as

$$\sum_{i=1}^{n} \$_i = 0 \tag{3}$$

where 0 is a vector of dimension equal to twist $\$_i$ dimension.

According to the normalized screw definition introduced above, Eq. (2) may be rewritten as

$$\sum_{i=1}^{n} \hat{\$}_i \dot{q}_i = 0 \tag{4}$$

where $\hat{\$}_i$ and $\dot{q}_i$ correspond respectively to the normalized screw and the magnitude of twist $\$_i$.

Equation (4) is the constraint equation, which can be written as

$$N\dot{q} = 0 \tag{5}$$

where $N=[\hat{\$}_1 \quad \hat{\$}_2 \quad ... \quad \hat{\$}_n]$ is the network matrix containing the normalized screws and $\dot{q} = [\dot{q}_1 \quad \dot{q}_2 \quad ... \quad \dot{q}_n]$ is the magnitude vector. The normalized screws have their signs dependent on the screw definition in the circuit orientation,

A closed kinematic chain has actuated joints, here named primary joints, and passive joints, named secondary joints. The constraint equation, Eq. (5), allows the calculation of the secondary joint velocities as functions of the primary joint velocities. To this end, the constraint equation is partitioned in primary and secondary quantities, resulting in

$$\begin{bmatrix} N_p & \vdots & N_s \end{bmatrix} \begin{bmatrix} \dot{q}_p \\ ... \\ \dot{q}_s \end{bmatrix} = 0 \tag{6}$$

where N_p and N_s are the primary and secondary network matrices, respectively, and $\dot{q}_p$ and $\dot{q}_s$ are the corresponding primary and secondary magnitude vectors.

Equation (6) can be rewritten as

$$N_p\dot{q}_p + N_s\dot{q}_s = 0 \tag{7}$$

The secondary joint position can be calculated by integrating Eq. (7) as follows:

$$q_s(t) - q_s(0) = \int_0^t \dot{q}_s dt = -\int_0^t N_s^{-1} N_p \dot{q}_p dt \tag{8}$$

2.3. Assur virtual chain

The Assur virtual kinematic chain concept, virtual chain for short, is essentially a tool to obtain information on the movement of a kinematic chain or to impose movements on a kinematic chain (Campos *et al*, 2005).

This concept was first introduced by Campos *et al* (2005), which defines the virtual chain as a kinematic chain composed of links (virtual links) and joints (virtual joints) which possesses the following three properties: a) the virtual chain is open; b) it has joints whose normalized screws are linearly independent; c) it does not change the mobility of the real kinematic chain.

From the c) property, the virtual chain proposed by Campos *et al.*(2005) is in fact an Assur group, i.e. a kinematic subchain with null mobility that when connected to another kinematic chain preserves mobility (Artobolevski, 1977).

To represent the movements in the Cartesian system the 3P3R virtual chain is used. This chain is composed of three orthogonal prismatic joints (in the *x*, *y*, and *z* directions), and a spherical wrist, which can be decomposed in three rotational joints (in the *x*, *y*, and *z* directions). Figure 2 shows the 3P3R Assur virtual chain with the virtual links C_i labeled.

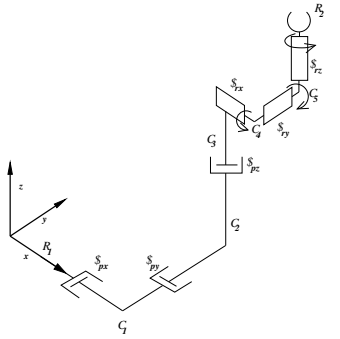

Figure 2. 3P3R Assur virtual chain.

Other Assur groups can be founded in Artobolevski (1977) and in Davidson and Hunt.(2004).

2.4. The direct graph notation

Consider a kinematic pair composed of two links E_i and E_{i+1}. This kinematic pair has its relative velocity defined by a screw ${}^{R}\$_j$ (joint j) relative to a reference frame R. Joint j represents the relative movement of the link E_i with respect to the link E_{i+1}. This relation can be represented by a graph, as shown Fig. 3(a), where the vertices represent links and the arcs represent joints. The relative movement is also indicated by the arcs directions. In Fig. 3(a), for instance, link E_{i+1} moves relative to link E_i via joint j.

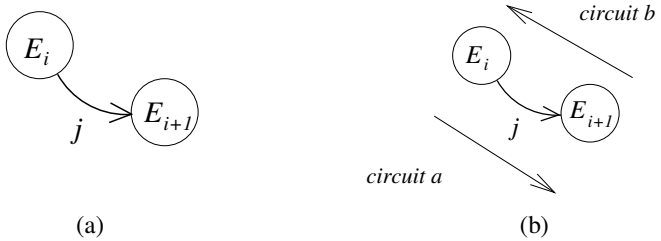

Figure 3. (a) Movement of link E_i relative to link E_{i+1};
(b) Relation between joint j and the *circuits a* and *b*.

Now consider the following example, where joint j is part of two closed chains. For each closed chain the circuit direction is defined (Campos *et al*, 2005). Figure 3(b) illustrates this case. In a direct mechanism graph, if the joint has the same direction as the circuit, the twist associated with the joint has a positive sign in the circuit equation (Eq. (13)), and a negative sign if the joint has the opposite direction to the circuit.

In the example, twist ${}^{R}\$_j$, associated with joint j will have a positive sign in *circuit a* equation and a negative sign in *circuit b* equation.

2.5. Integration algorithm using Assur virtual chains

Simas (2008) and Simas *et al* (2009) present a new integration algorithm to obtain joint positions from the differential kinematics equation. The algorithm proposed has two steps. The first step is to introduce a virtual chain to represent the closure error. The constraint equation of this closed-loop chain results in

$$N_p\dot{q}_p + N_s\dot{q}_s + N_e\dot{q}_e = 0 \tag{9}$$

where N_p and N_s are the primary and secondary network matrices obtained by integration, $\dot{q}_p$ and $\dot{q}_s$ are the primary and secondary magnitude vectors, N_e is the error network matrix and $\dot{q}_e$ is the error magnitude vector.

The second step is to isolate the secondary magnitude vector to replace Eq. (9) by

$$\dot{q}_s = -N_s^{-1}N_p\dot{q}_p + N_s^{-1}N_eK_eq_e \tag{10}$$

where the gain matrix K_e is chosen to be positive definite and q_e is the position error vector.

Applying the Euler integration method in Eq. (10) results in

$$q_s(t_k) = q_s(t_{k-1}) - N_s^{-1}(t_{k-1})N_p(t_{k-1})\dot{q}_p\Delta t + N_s^{-1}(t_{k-1})N_e(t_{k-1})K_eq_e\Delta t \tag{11}$$

The proposed method is stable and allows execution of several iterations until the error is within the admissible tolerance (Simas, 2008). To use this proposed method it is necessary to obtain the position error vector.

2.6. Position error vector

Screw displacement of a link in a kinematic chain can be expressed by a homogeneous matrix, and the resultant screw displacement in a link j can be calculated using the successive screw displacements method by premultiplying the homogeneous matrices corresponding to the preceding joint motions, i.e.

$$A_j = \prod_{i=1}^{j-1} A_i \tag{12}$$

As in a closed loop chain, the first and the last links are the same, and the orientation and position of a link with respect to itself is an identity matrix. In a closed-loop chain with *np* primary joints and *ns* secondary joints, Eq.(12) can be rearranged, resulting in

$$\prod_{i=1}^{np}[A_p]_i \prod_{i=1}^{ns}[A_s]_i = I \tag{13}$$

where $[A_p]_i$, $i = 1\ldots np$ are the homogeneous matrices corresponding to the primary joints and $[A_s]_i$, $i = 1\ldots ns$ are the homogeneous matrices corresponding to the secondary joints.

We represent the closure error with a homogeneous matrix E, and the closed-loop equation becomes

$$\left\{\prod_{i=1}^{np}[A_p]_i \prod_{i=1}^{ns}[A_s]_i\right\}E = I \tag{14}$$

The closure error is calculated by

$$E = \left\{\prod_{i=1}^{np}[A_p]_i \prod_{i=1}^{ns}[A_s]_i\right\}^{-1} = \begin{bmatrix} R_e & p_e \\ 0 & 1 \end{bmatrix} \tag{15}$$

where p_e=[p_{ex} p_{ey} p_{ez}]^T is the position error vector and R_e is the rotation matrix error. The matrix R_e corresponds to the error measured in r_{ex}, r_{ey} and r_{ez} virtual rotative joints considering their structural conception.

The "position" error (which is a posture error involving position and orientation) is given by the position error vector q_e=[r_{ex} r_{ey} r_{ez} p_{ex} p_{ey} p_{ez}]^T.

3. DIFFERENTIAL KINEMATICS MODELS

3.1. Eclipse and Eclipse-II kinematic structures

The Eclipse kinematic design consists of three *PPRS* serial chains (where *P*, *R*, and *S* denote prismatic, revolute, and spherical joints, respectively). The first *P* joint performs sliding motion along the circular guideway. This robot has six degrees of freedom, where the prismatic joints are the actuated ones (Park, 2001). The three kinematic subchains are connected to a triangular moving plate through *S* joints. Figure 4 depicts this structure, where *a*, *b*, *c* identify each subchain and p_{cj}, p_{vj}, r_j, s_j denotes the circular prismatic, vertical prismatic, rotative and spherical joints, respectively.

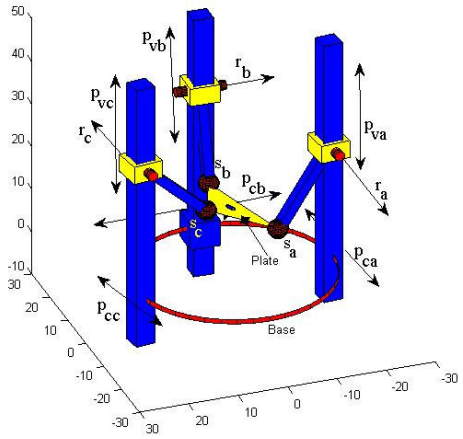

Figure 4. Eclipse kinematic design.

The Eclipse-II kinematic design is also composed by three *PPRS* serial subchains, moving independently along a fixed circular guide. Differently from the Eclipse robot, one subchain has a circular prismatic chain substituting the vertical prismatic joint. This modification results in a large orientation workspace, as can be seen in Figure 5. This second circular prismatic joint in one subchain is identified by p_{ha}.

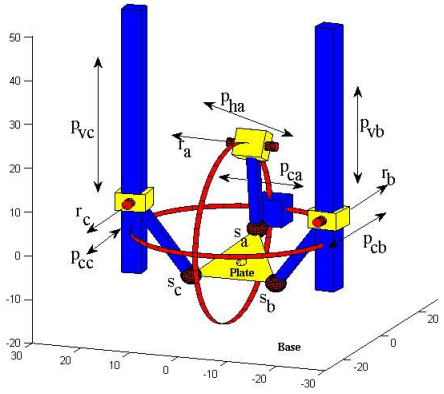

Figure 5. Eclipse-II kinematic design.

3.2. Differential kinematics modeling

It was observed that Eclipse and Eclipse-II robots have the same graph model, resulting in the same Davies equation. The only difference is in the screw definition of the second prismatic joint of one of the subchains, as explained in the previous section. To impose movement to the moving plate, an Assur virtual chain were added. There were added error virtual chains for each circuit composed of the subchains. Figure 6 shows the resulting graph.

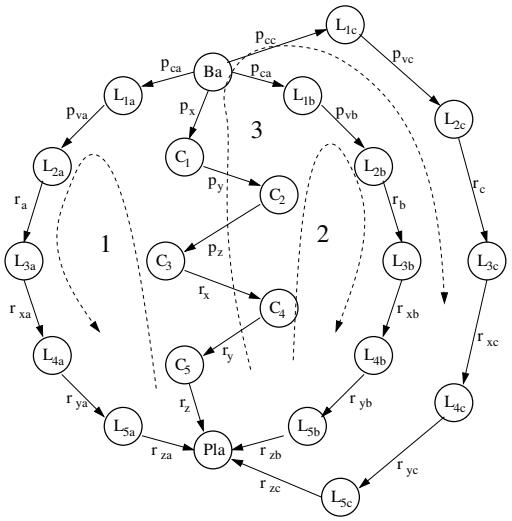

Figure 6. Eclipse and Eclipse-II graph

In this figure, L_{ij} denotes *i-th* link of *j* subchain. p_{cj}, p_{vj}, r_j are the prismatic circular joint, the prismatic vertical joint and the revolute joint of *j* subchain, respectively. In the graph, spherical joints are replaced by three rotative joints r_{xj}, r_{yj}, r_{zj} to represent movement in each orthogonal direction.

From the graph and the joint arrangements, N_p and N_s matrices are determined, and the constraint equations for each robot configuration are obtained. Equation (16) corresponds to the Eclipse constraint equation.

$$N_s\dot{q}_s + N_p\dot{q}_p = \begin{bmatrix} M_a & 0 & 0 \\ 0 & M_b & 0 \\ 0 & 0 & M_c \end{bmatrix}\begin{bmatrix} \psi_a \\ \psi_b \\ \psi_c \end{bmatrix} + \begin{bmatrix} M_{ta} & 0 & 0 \\ 0 & M_{tb} & 0 \\ 0 & 0 & M_{tc} \end{bmatrix}\begin{bmatrix} \psi_{ta} \\ \psi_{tb} \\ \psi_{tc} \end{bmatrix} = 0 \tag{16}$$

In Eq. (16), each *M* matrix corresponds to a set of unitary screws. $M_j = \left[\hat{\$}_{cj} \quad \hat{\$}_{vj} \quad \hat{\$}_{rj} \quad \hat{\$}_{xj} \quad \hat{\$}_{yj} \quad \hat{\$}_{zj}\right]$ is related to the *j* subchain, while $M_{tj} = \left[\hat{\$}_{px} \quad \hat{\$}_{py} \quad \hat{\$}_{pz} \quad \hat{\$}_{rx} \quad \hat{\$}_{ry} \quad \hat{\$}_{rzj}\right]$ is related to the virtual chain that imposes the trajectory of each eclipse subchain. Vectors ψ_j and ψ_{tj} are formed by magnitudes of the velocities of each chain. It should be noted that the first five screws of the Assur virtual chains that define trajectories are the same for the Eclipse subchains *a*, *b* and *c*, while the sixth screw differs in each case, because of the shape of the end-effector plate. Since the model in this work considers this plate as equilateral triangular, each $\hat{\$}_{rzj}$ corresponding magnitude has a phase angle of 0°, 120° or -120° summed to it.

Eclipse-II has same constraint equation structured as Eclipse, changing only the screw $\hat{\$}_{va}$ for the screw $\hat{\$}_{ha}$, according to the joint change explained in the previous section.

4. SINGULARITY ANALYSIS

Kim and Park (1998) and Kim *et al* (2002) discuss the complexity of kinematics in Eclipse and Eclipse-II, respectively. Their studies were based on geometric analysis and numerical approaches. Alternatively, the singularity conditions for forward and inverse kinematics can be determined from the model presented on the previous section.

4.1 Inverse singularity analysis

In Eq. (16), it can be noted that the secondary matrix is constituted of a set of submatrices disposed along the principal diagonal. So, inverse kinematic singularities can be evaluated by calculation of the determinant of the M_j submatrix, which has the same structure for each subchain, as shown in Equation (17), where q_{rj} is the angle of the joint r_j, r is the length of the link which connects vertical prismatic joint p_{vj} and spherical joint s_j and r_g is the distance from the base to the circular guide.

$$D(M_j) = r(-r_g + r\cos(q_{rj}))\cos(q_{yj})\sin(q_{rj}) \tag{17}$$

From Eq. (17), it can be observed that singularity conditions occur on the following conditions:

- q_{rj}=0 rad;
- q_{yj}=π/2 rad;
- $r\cos(q_{rj})$=r_g.

These conditions are the same for each subchain of Eclipse and for *b* and *c* subchains of Eclipe-II. For the *a* subchain of Eclipse-II, the determinant results in

$$D(M_a) = r_g r\left(-r_g\cos\left(\frac{L_a}{r_g}\right) + r\cos\left(q_{ra} + \frac{L_a}{r_g}\right)\right)\cos(q_{ya})\sin(q_{ra}) \tag{18}$$

where L_a is the displacement of the p_{ha} joint.

According to Eq. (18), the *a* subchain has the following singularity conditions:

- q_{ra}=0 rad;
- q_{ya}=π/2 rad;
- $r\cos\left(q_{ra} + \frac{L_a}{r_g}\right) = r_g\cos\left(\frac{L_a}{r_g}\right)$

4.1 Direct singularity analysis

In Eq. (16), it can be observed also that the primary matrix is constituted of submatrices along its main diagonal. Direct kinematic singularities can be evaluated by calculating the determinant of the M_{ti} submatrix, which has the same structure for each subchain. This determinant is shown in Eq. (19), where q_{dy} is the desired displacement of the r_y rotative joint of the virtual *3P3R* trajectory generator chain.

$$D(M_{ti}) = -\cos(q_{dy}) \tag{19}$$

From Eq.(19), singularity occurs when $q_{dy}=\pi/2$.This result is applicable for both Eclipse and Eclipse-II.

The results obtained here can solve both direct and inverse kinematics, by use of the numerical algorithm presented in Eq. (16). The next section presents numerical simulations to illustrate the method for Eclipse and Eclipse-II.

5. EXPERIMENTAL SIMULATION

To perform numerical simulations the following dimensions were adopted:

- r_g=20 *cm*
- r=20 *cm*
- Equilateral triangular plate with side = $10\sqrt{3}$ *cm*

The 3-dimensional trajectory was composed of 100 points, and it consisted of an ellipse defined on *XY* plane together with a sinusoidal movement in *Z* axis. Orientation was maintained constant, according to Eq. (20).

$$Traj(t)=\begin{cases} x(t)=5\cos(2\pi t) \\ y(t)=3\sin(2\pi t) \\ z(t)=10+\sin(6\pi t) \\ \phi_x=0.5rad \\ \phi_y=0rad \\ \phi_z=0.1rad \end{cases} \quad \text{with} \quad 0\le t\le 1 \quad \text{and} \quad \Delta t=0.01 \tag{20}$$

where *x(t), y(t)* and *z(t)* are parametric functions that defines the displacements to the prismatic joints of the Assur virtual trajectory chain, and ϕ_x, ϕ_y and ϕ_z are the desired angular position to the rotative joints of the Assur virtual trajectory chain.

Trajectory is shown in the Fig. 7. Figure 8 depicts a sequence of eight configurations of the Eclipse robot while the end-effector follows the trajectory.

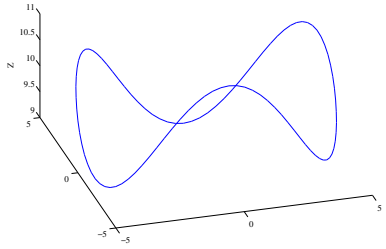

Figure 7. Programmed trajectory to Eclipse and Eclipse-II

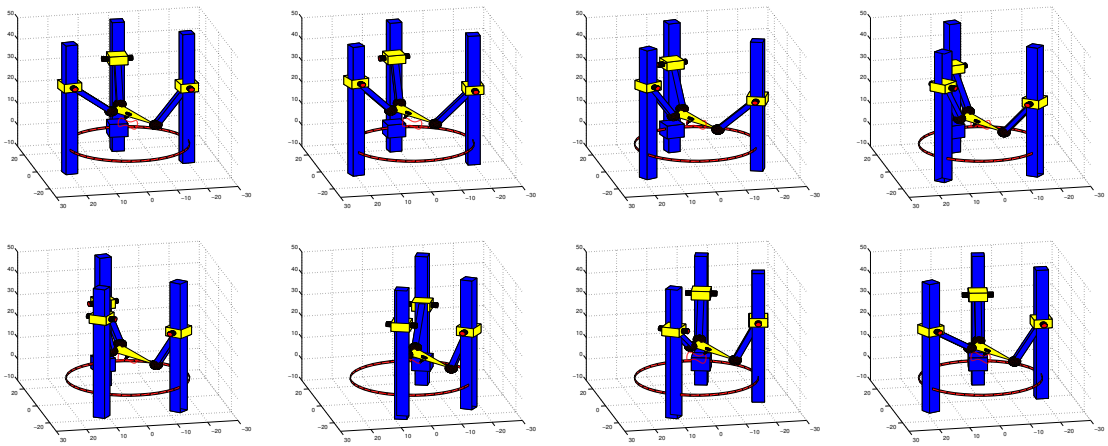

Figure 8. Sequence of eight positions of the robot Eclipse following the planned trajectory

It should be noted that the end-effector movement is performed by the displacement of the vertical prismatic joints and its vertical support columns over the circular guide.

Figure 9 presents the profiles of prismatic joints position for the circular guide ring and for the vertical columns.

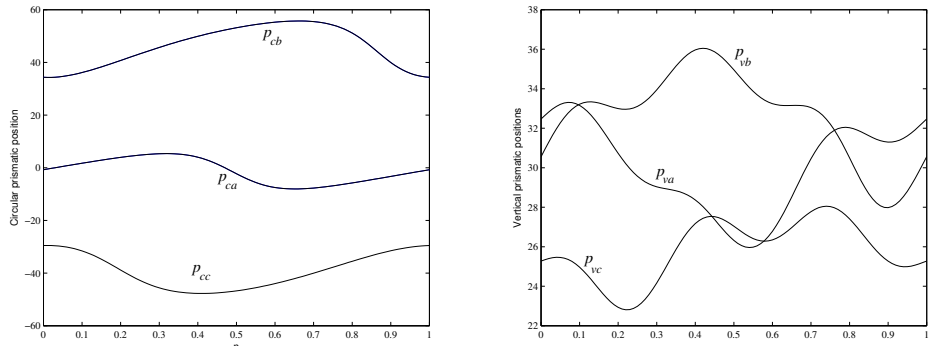

(a) (b)

Figure 9. Prismatic joint position: (a) circular guide prismatic joint; (b) vertical prismatic joint

The same trajectory was imposed to the end-effector of Eclipse-II robot. Figure 10 presents a sample of eight configurations of its kinematic chain, while executing the task imposed to it.

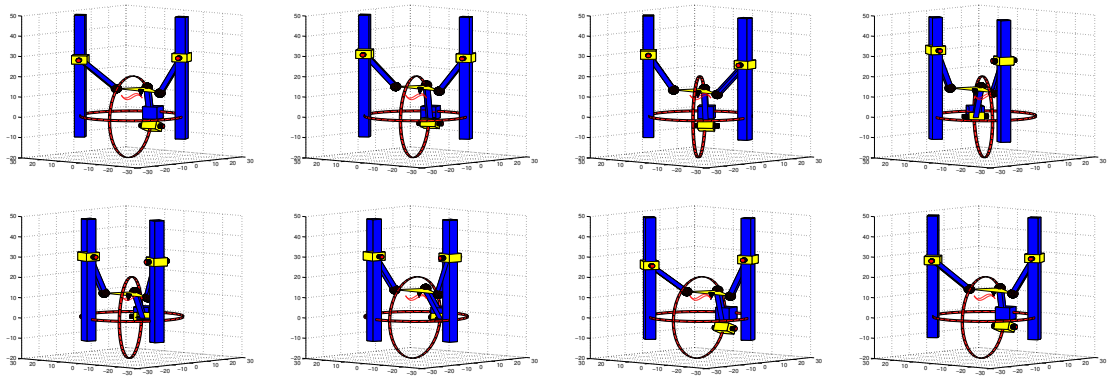

Figure 10. Sequence of eight positions of the robot Eclipse-II following the planned trajectory

Similar to Eclipse, the movement of the end-effector is performed by displacement of the three vertical prismatic joints (including the vertical prismatic joint with circular guide), and its respective columns movements in relation with the circular guide in the base. Figure 11 presents the profiles of prismatic joints position of the circular guide ring and of the vertical columns to Eclipse-II.

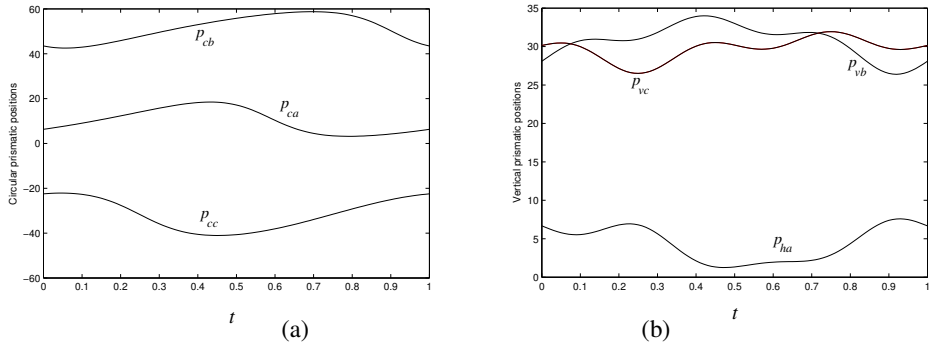

(a) (b)

Figure 11. Prismatic joint position to Eclipse-II: (a) circular prismatic joint;
(b) vertical prismatic joints and circular prismatic joint p_{ha}

Copyright © 2009 by ABCM

3. CONCLUSION

This paper presented an alternative kinematic differential model for the Eclipse and Eclipse-II parallel robots. The model discussed was based on Assur virtual chains, and its development followed a systematic way, which is a characteristic of this method. An integration method with closure error control was employed in order to compute the joints positions and so, the references for the robots' actuators. The results originated the implementation of an algorithm for trajectory generation concerning inverse and forward singularity condition.

The method will be applied to other complex robot architectures, like Adept® Quattro, and PKM® Tricept, and the results will be presented in future work.

4. REFERENCES

Altuzarra, O., Pinto, C., Avilés, R. and Hernández, A., 2004, "A Practical procedure to analyze singular configurations in closed kinematic chains", IEEE Trans. on Robotics, Vol 20, No 6.

Artobolevski, I.I., 1977 "Théorie des Mécanismes et des Machines", Mir Publishers, Moscow.

Campos, A.,Guenther R. and Martins D., 2005, "Differential kinematics of serial manipulators using virtual chains," J. Brazilian Soc. Mechanical Sciences & Engineering, Vol 27, No 4, pp. 345-356 .

Davidson, J. K. and K.H. Hunt, 2004, "Robots and screw theory: applications of kinematics and statics to robotic", Oxford University Press Inc, New York.

Gosselin, C. and Angeles, J., 1990, "Singularity Analysis of Closed-Loop Kinematic Chains", IEEE Trans. on Robotics and Automation, Vol 6, No 3, pp-281-290.

Gregorio, R. ,2005, "Forward problem singularities in parallel manipulators which generate SX–YS–ZS structures", Mechanism and Machine Theory, Vol 40, No. 5, pp. 600–612.

Kim, J. and Park, F.C., 1998, "Eclipse: A new parallel mechanism prototype", Position Paper in Proc First European American Forum on Parallel Kinematic Machines, Milan, Italy.

Kim, J., Hwang, J. C., Ki, J. S., Iurascu, C. C., Park, F. C. and Cho, Y. M., 2002, "Eclipse II: A New Parallel Mechanism Enabling Continuous 360-Degree Spinning Plus Three-Axis Translational Motions", IEEE Trans. on Robotics and Automation , Vol. 18, No 3, pp. 367-373.

Liu, G., Lou, Y. and Li, Z., 2003, "Singularities of Parallel Manipulators: A Geometric Treatment", IEEE Trans. on Robotics and Automation, Vol 19, Issue 4**,** pp-579-597.

Simas, H., 2008, "Planejamento de trajetórias e evitamento de colisão em tarefas de manipuladores redundantes operando em ambientes confinados". PhD thesis, Universidade Federal de Santa Catarina.

Simas, H., Guenther, R., da Cruz, D. F. M. and Martins, D., 2009, "A new method to solve robot inverse kinematics using Assur virtual chains", Robotica, (Cambridge), doi:10.1017/S0263574709005426.

Wang, Y., 2006, "An Incremental Method for Forward Kinematics of Parallel Manipulators", Proc. of the IEEE International Conference on Robotics, Automation and Mechantronics, Bangkok, Thailand, pp. 243-247.

5. RESPONSIBILITY NOTICE

The authors are the only responsible for the printed material included in this paper.